

## Properties and synthesis of ultra-thin SOFC structures

Jingyu Shi, Frank M. Zalar, and Henk Verweij

*Department of Materials Science & Engineering, Ohio State University, 2041 College Road, Columbus OH 43210-1178, USA*

*Internet: [www.mse.eng.ohio-state.edu/fac\\_staff/faculty/verweij/](http://www.mse.eng.ohio-state.edu/fac_staff/faculty/verweij/)*

### Abstract

This paper presents an initial exploration of the use and possibility of nm thin SOFC electrolyte structures to enhance cell performance. This is addressed, on one hand, by analyzing the extent of interfacial space-charge areas at the electrode-electrolyte interface. A simple thermodynamic treatment shows that such areas have a characteristic dimension in the order of 0.2 nm so that they can be classified as 2D interfacial effects and will not affect bulk electrolyte behavior. The characteristic dimensions may appear to be larger in more advanced treatments of restricted statistical distribution of charge carriers over the electrolyte lattice. On the other hand it is shown that 10 nm thin, dense zirconia layer can be prepared, here by spin coating of <10 nm spherical zirconia particles onto silicon substrates, followed by O<sub>2</sub> plasma treatment and annealing at 600°C. This unconventional strategy can also be used to realize foreseen, ideal graded electrode structures, in combination with thin electrolytes.

### Introduction

State-of-the-art Solid Oxide Fuel Cell (SOFC) designs have a dense, oxygen ion conducting solid electrolyte sandwiched between mixed-conducting electrodes which may be dense, porous, and/or composite. The most commonly used materials for SOFC are Ytria-stabilized Zirconia (YSZ) as electrolyte, Lanthanum-Strontium Manganate as cathode and Ni-YSZ composite as anode [1-3]. SOFC charge transfer reactions are generally assumed to occur at triple-phase-boundaries (TPB's) between electrode, electrolyte and gas phase. The efficiency of SOFC conversion is most likely affected by:

- Resistive losses in the bulk electrolyte, including constriction effects due to the fact that charge transfer occurs at narrow TPB's only.
- Surface charge transfer at the TPB.

The effective thickness of the TPB is generally assumed to be in the order of 10 nm. This naturally leads to the suggestion that typical dimensions of cathode and anode material and porosity should also be of the order of 10 nm to obtain the best possible electrode efficiency. In the ideal electrode/electrolyte interface there are many active triple phase boundary contacts, possibly percolating into the porous electrode structure. Further away from the electrolyte interface, both cathode and anode may coarsen to allow for an optimum strength, gas transport and electron conductivity.

The minimum electrolyte thickness is also estimated to be in the order of 10 nm, which is just one order of magnitude larger than unit cell dimensions. Such a thickness is achievable by stretching the limits of what is possible with high definition colloidal processing. However, one of the concerns is that in very thin electrolyte structures, ion-conductivity changes from the bulk value. Although a lot of work has been done toward improving the overall performance of SOFCs through the use of various materials and design modifications, a comprehensive detailed description of transport in SOFCs is lacking in the literature. The best example known to the authors describes the defect concentration and electrostatic potential in the interfacial

regions inside of a thick solid electrolyte (2 mm) [4]. Unaddressed are the effects upon the interfacial regions for very thin electrolytes.

This paper presents initial results of integrated modeling and synthesis efforts to support design and manufacturing ultra-thin electrolyte structures. A finite element description is presented of the concentration of solid state charge carriers, based on Langmuir lattice statistics, and solving the Poisson equation. In addition, an unconventional route is presented towards thin electrolyte structures by synthesis and consolidation of <10 nm spherical zirconia particles by modified emulsion precipitation.

## Experimental

**Modeling.** An equilibrium description for charge carriers ( $l = O^{2-}$ ) in the electrolyte was formulated from the Poisson equation (1) and an expression for electrochemical potential, that in its most simple form appears as (2):

$$-\nabla^2 \varepsilon \Phi = \rho_q \quad (1)$$

$$\tilde{\mu}_l = \mu_l^0 + k_B T \ln \left( \frac{\theta_l - \theta_l^{\min}}{\theta_l^{\max} - \theta_l} \right) + z_l q_{el} \Phi \quad (2)$$

The entropic term of the electrochemical potential is based upon an ideal Langmuir lattice and considers site exclusion. The variable  $\theta_l$  is the local occupied fraction of lattice sites for the species  $l$ .  $\theta_l^{\max}$  and  $\theta_l^{\min}$  are an empirical terms that are 1 and 0, respectively in an ideal Lanmuir lattice. They account for configuration restrictions, imposed by the lattice, on the minimum number if anions, surrounding a cation. The charge density term in the Poisson equation,  $\rho_q$ , is a function of  $\theta_l$ , expressed as the relative volumetric excess or deficiency of carriers of species  $l$  as compared to the bulk,  $\rho_q = Q(\theta_l - \theta_l^0)$  where  $Q$  is a constant. Since in equilibrium the gradient in electrochemical potential equals zero,  $\nabla \tilde{\mu} = 0$ , an expression for  $\theta_l$  in terms of the electrostatic potential  $\Phi$  is obtained using the nominal bulk concentration and zero electrostatic potential as reference points. This expression is then used in the Poisson equation to produce an equation in one variable. FEMLAB® (v. 3.0a) software was used to solve this nonlinear form of the Poisson equation for yttria-stabilized zirconia electrolytes of varying thick/thinness.

To obtain more sophisticated expressions for restrictions, imposed by the lattice, a program was written in MapleV® (v. 9) software for generating and evaluating random defect structures. Virtual crystals were built of three cubic YSZ unit cells on each edge resulting in 108 zirconium ion sites and 216 oxygen ion sites constituting the Langmuir lattice. The crystals were generated first with an electroneutrality constraint and then without. The resultant crystals were then inspected for conformation to a set of configurational constraints. Zirconium ions were required to be coordinated by at least seven oxygen ions, and yttrium ions by at least five oxygen ions. (Other constraints may follow from a detailed comparison with experimental data.) For each set of parameters – doping level and number of vacancies – 100 virtual crystals were generated and the number of valid configurations recorded. This was repeated 5 times for each data point.

**Nanoparticles and thin electrolyte synthesis.** Zirconia nanoparticles were synthesized by a modified emulsion precipitation method (MEP) [5,6]. Two water-in-oil emulsions were prepared by dispersing 0.04M zirconium chloride or 0.05M

hexamethylenetetramine (HMTA) aqueous solutions as droplets in decane by using nonylphenol tetraethyleneglycol ether (Arkopal 40) as surfactant, didodecyldimethylammonium bromide (DiDAB) as co-surfactant, and an Ultra-Turrax dispersion tool (T25, IKA). Both emulsions were mixed and heated for 15 minutes at 60°C while stirring to decompose HMTA into ammonia and formaldehyde. It is believed that the frequent collision of aqueous droplets and exchange through the, temporarily, common surfactant membrane lead to a precipitation reaction between zirconium ions and ammonia, resulting in the formation of zirconium hydroxide inside the aqueous droplets. Poly-octadecyl methacrylate (PODMA) was added as a steric stabilizer, followed by water removal via azeotropic distillation, to achieve steric stabilization of the nanoparticles in the eventual oil phase. A transparent dispersion of precursor oxide nanoparticles in decane was obtained after the distillation of water and the precipitation of NH<sub>4</sub>Cl and DiDAB.

To enable the preparation of a thin, fully dense ZrO<sub>2</sub> electrolyte layer, a purified dispersion was deposited onto silicon substrates by spin coating with a P6700 spin coater. After drying at room temperature, the coating was heated at 200°C for 3 hours, followed by oxygen plasma treatment to remove organic residuals and then heated to develop the crystallized structure. The precursor nanoparticles and the coating cross-sections were examined by a transmission electron microscopy (Philips CM200) with an accelerating voltage of 200 KV. Nanoparticle samples were prepared by directly applying a purified dispersion on a carbon coated Cu grid and dried at room temperature. The cross-section samples of the coatings were prepared by Focused Ion Beam (Dual Beam 235 FIB, FEI) cutting. Carbon was deposited on the coated wafer surface as a conductive layer during FIB sample preparation.

## Results and discussion

**Modeling.** In figure 1, are presented plots of electrostatic potential,  $\Phi$ , and the fractional carrier site occupancy,  $\theta_i$ , as functions of position for a 1 nm thick YSZ electrolyte in equilibrium condition. The nominal bulk occupation of carrier sites,  $\theta_i^0$ , was taken as 0.5, and the bulk reference electrostatic potential was taken as 0 V. Values for  $\theta_i^{\max}$  and  $\theta_i^{\min}$  were taken as 0.875 and 0.125, respectively. A 1 V potential was applied symmetrically across the electrolyte.

It can be seen in the plots that there is a space charge region on the order of 0.3 nm at the interfaces. This number is smaller than unit cell dimensions and hence indicates that the continuum approach, presented above, is not accurate. Because the order of magnitude is still correct, we keep using it because it enables a quick inventory for a wide range of models. The narrow space charge regions do not appreciably overlap, even for this 1 nm thin electrolyte and can be considered primarily as an interfacial effect. As the electrolyte is made thicker, the interfacial regions remain of the same size indicating that their width is likely most dependent

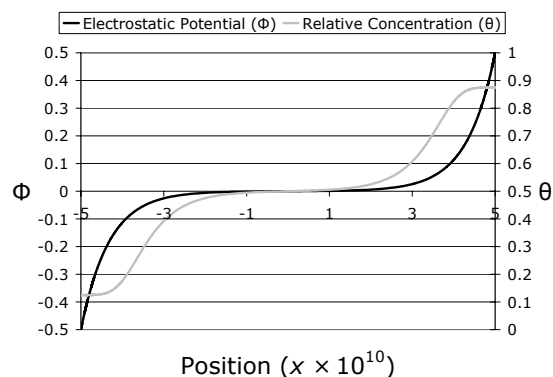


**Figure 1:** 1-D plots of FEMLAB® results for a 1 nm thick, heavily doped YSZ electrolyte showing the local electrostatic potential and the local fractional carrier site occupancy as functions of position.

upon the doping level. Our initial calculations show that, disregarding surface relaxation near the interface, electrolytes with >10 nm thickness will have bulk properties. The picture changes to some extent when configuration restrictions upon the fractional occupancy, and lower vacancy concentrations are considered. Configuration restrictions can be addressed by numerical simulation, as shown below.

Random “virtual” crystals were generated with a pre-specified doping level and electroneutrality enforced. These “virtual” crystals were then inspected with respect to allowed configuration criteria as presented before. In figure 2, results of this exercise are presented. The data points are the average of 5 replications, and the error bars are 1 standard deviation of the replications. The fit curve is a 3 parameter sigmoidal function (3):

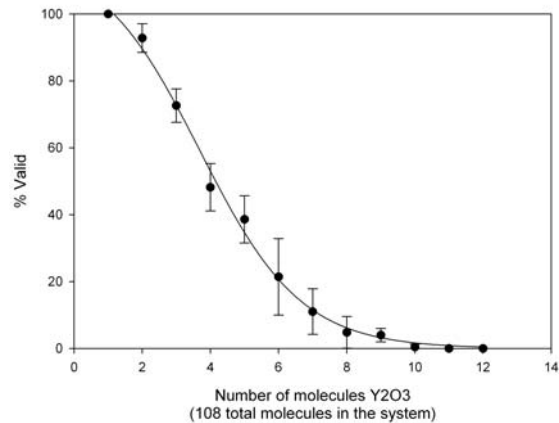
$$y = \frac{a}{1 + \exp\left(\frac{-(x - x_0)}{b}\right)} \quad (3)$$

where  $a$ ,  $b$ , and  $x_0$  are the fit parameters.

For random configurations, the results indicate that the number of valid configurations decreases rapidly as the number of vacancies present increases. This has an impact on the configurational entropy of the system and the mobility of carriers. The effect of reducing configurational entropy leads to widening of the space charge areas.

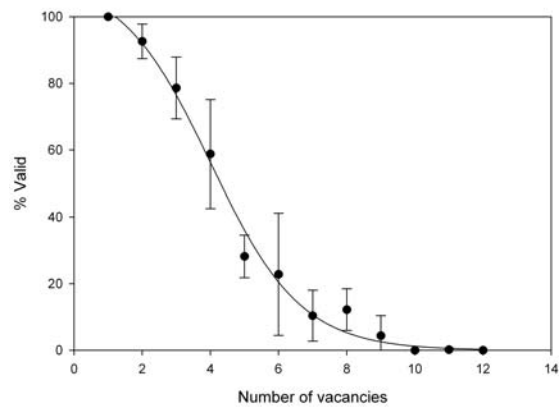
In figure 3, results similar to those in the previous figure are presented. In this case, however, electroneutrality is not enforced, and the crystal is doped with 20 yttrium ions on a total of 108 sites. As the number of vacancies is increased the number of valid configurations again decreases rapidly. Similar results were observed with other doping levels (6-18 yttrium ions).

It should be noted that the number of replications is rather low (5) in these data. Also, these configurations were derived completely randomly, whereas, vacancies are likely attracted to the yttrium ions more so than to the zirconium ions. This vacancy binding is the subject of further investigation, and is possibly incorporated in further configuration restrictions. It is also the subject of further investigation to examine the effect of configuration restrictions on transport mobility.



$a$	$b$	$x_0$	$R^2$
118.2207	-1.4849	3.6929	0.9962

**Figure 2:** Plot of “virtual” crystal data with enforced electroneutrality condition.



$a$	$b$	$x_0$	$R^2$
112.2579	-1.3292	4.0065	0.9915

**Figure 3:** Plot of “virtual” crystal data without electroneutrality condition. The crystal was doped with 20 yttrium ions on a total of 108 sites.

**Nanoparticles and thin electrolyte synthesis.** Figure 4 shows a TEM micrograph of  $ZrO_2$  precursor nanoparticles obtained by the MEP method. The particles appear spherical in morphology, non-agglomerated and with a narrow size distribution of 5 nm in diameter. The preparation of a dense zirconia electrolyte of 10 nm in thickness can be accomplished by depositing a thin layer of 5 nm zirconia nanoparticles, followed by densification and crystallization. Since the particles are covered with a steric stabilizer layer and well dispersed in decane, they can move independently of each other during the layer formation without the occurrence of agglomeration. This will result in a random-close-packed structure in the as-deposited coating after the evaporation of dispersion medium at 200°C. The complete densification of random-close-packed, polymer-stabilized spherical 5 nm zirconia particles can take place at near room temperature by oxygen plasma treatment, as shown in figure 5.

A  $ZrO_2$  coating, prepared by spin coating and annealing at 600°C was characterized by TEM of a cross-section sample, see figure 6. The 10 nm thickness of the  $ZrO_2$  coating was homogenous on the scale of observation. The coating appears dense and adheres very well to the substrate. Work is in progress to characterize the grain structure of the coating by HRTEM.

### Conclusions

- An equilibrium model based on electrochemical potential and the Poisson equation indicates that space charge regions of a YSZ electrolyte may be on the order of 2 to 3 Å.
- Computer simulation of random defect structures in “virtual” crystals shows a strong impact on configurational entropy as vacancy concentration increases to modest values of a few percent. This effect may lead to wider space charge areas that become more of the order of 10 nm thin electrolyte structures.
- The imposed configuration limitations also present additional obstacles to carrier mobility.
- Non-agglomerated ~5 nm Ø  $ZrO_2$  nanoparticles were synthesized successfully via modified emulsion precipitation. The particles obtained have a spherical shape and narrow size distribution.
- Preliminary results showed that a dense, homogeneous  $ZrO_2$  coating of 10 nm in thickness could be made by spin coating a silicon wafer substrate with a purified  $ZrO_2$  nanoparticle dispersion. The densification temperature was greatly reduced due to the small particle size and the homogeneous packing of the initial stabilized nanoparticles.

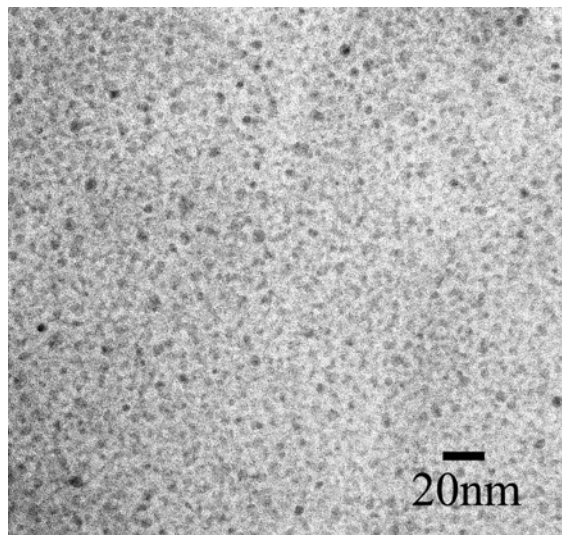


**Figure 4:** TEM image of non-agglomerated  $ZrO_2$  precursor nanoparticles.

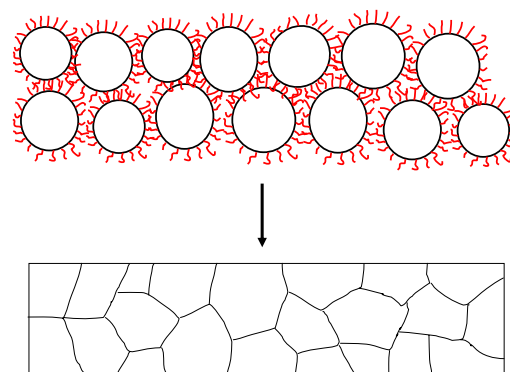


**Figure 5:** Proposed densification of random-close-packed nanoparticle ensemble, initiated by oxygen plasma treatment.

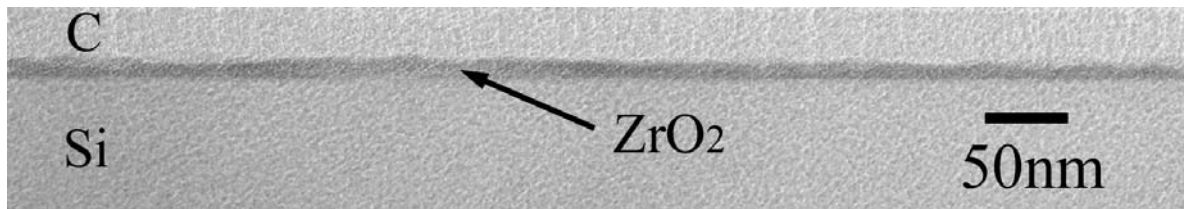


**Figure 6:** Cross-sectional TEM image of a ZrO<sub>2</sub> coating prepared by spin coating and annealed at 600°C.

## References

1. B.C.H. Steele and A. Heinzl, "Materials for fuel-cell technologies," *Nature*, **414** 345-52 (2001).
2. J. Will, A. Mitterdorfer, C. Kleinlogel, D. Perednis and L.J. Gauckler, "Fabrication of thin electrolytes for second-generation solid oxide fuel cells," *Solid State Ionics*, **131** 79-96 (2000).
3. E. Ivers-Tiffée, A. Weber and D. Herbstritt, "Materials and technologies for SOFC-components," *J. Eur. Ceram. Soc.*, **21** 1805-11 (2001).
4. S.F. Potamianou and K.A.Th. Thoma, "A study of ion transport in zirconia through computer modeling," *Solid State Ionics*, **70/71** 533-536 (1994).
5. F.C.M. Woudenberg, W.F.C. Sager, N.G.M. Sibelt and H. Verweij, "Dense nanostructured t-ZrO<sub>2</sub> coatings at low temperatures via modified emulsion precipitation," *Adv. Mater.*, **13** [7] 514-16 (2001).
6. W.F.C. Sager, H.F. Eicke and W. Sun, "Preparation of nanosized uniform ceramic particles in emulsions," *Colloids and Surfaces A*, **79** 199-16 (1993).